

Structure effect of some thiosemicarbazone derivatives on the corrosion inhibition of $\text{Fe}_{78}\text{B}_{13}\text{Si}_9$ glassy alloy in Na_2SO_4 solution

S.T. Arab^a, K.M. Emran^{b,*}

^a Girls' College of Education, General Presidency of Education, P.O(55002), Jeddah 21413, Saudi Arabia

^b Girls' College of Education, General Presidency of Education, Al-Madinah Al-Monawarah, Saudi Arabia

Received 12 June 2006; accepted 28 May 2007

Available online 27 July 2007

Abstract

The corrosion and corrosion inhibition of $\text{Fe}_{78}\text{B}_{13}\text{Si}_9$ glassy alloy by some thiosemicarbazone derivatives in 0.2 M Na_2SO_4 solution containing 10% MeOH has been studied. Inhibitors efficiency was estimated from electrochemical (polarization and impedance) measurements. Nearly identical results obtained from both techniques and morphological study are consistent. The thiosemicarbazone derivatives gave maximum corrosion inhibition of the alloy in 0.2 M Na_2SO_4 solution and evidence to act as mixed inhibitors. Interestingly the corrosion of iron-base alloy was almost controlled by charge transfer process but sometimes it was controlled by diffusion. This has been explained in basis of impedance data and literature work. A correlation between the efficiency of corrosion inhibition and their molecular structure was established. A schematic represent model of adsorbed molecule on the alloy surface was suggested. Experimental results fitted the kinetic–thermodynamic isotherms. Negative values of ΔG_{ads}^0 were obtained for the compounds from potentiodynamic polarization and impedance studies indicated the spontaneous adsorption of inhibitors on the alloy and the value of active sites are approximately equal to unity. Linear free energy relationships (LFER) have been used to correlate the inhibition of benzaldehyde thiosemicarbazone and its *p*-substituted derivatives with the Hammett substitute constant (σ), the small positive slope (ρ) of the correlation line ($\rho=0.32$) shows a weak dependence of the adsorption character of the reaction center on the electron density of the ring.

Crown Copyright © 2007 Published by Elsevier B.V. All rights reserved

Keywords: Metallic glasses; Iron-base alloy; Corrosion, Inhibition; Structure effect; Electrochemical methods

1. Introduction

Metallic glasses are described as one of the metal alloys, they consist a new class of materials included at least one transition or noble metal and one or more metalloids (boron, carbon, phosphorus, silicon, ...etc.) [1]. The interest in iron-base glassy alloys is both scientific [2–4] and technological for the ever growing use of metallic glasses in the production of magnetic devices in transformers, recorders...etc. [5–7]. However, $\text{Fe}_{78}\text{B}_{13}\text{Si}_9$ glass was found suitable for use in distribution, power transformers and in motors because of extremely low core loss [8].

The corrosion of iron-base glassy alloys has been studied in different media [9–13]. $\text{Fe}_{78}\text{B}_{13}\text{Si}_9$ metallic alloy often does not form passive films in aggressive environments and therefore it is essential to control the corrosion of this alloy by some means, the use of inhibitors is one of these ways, which is widely used to control the corrosion of metallic materials [14]. Several studies investigated the inhibition effect of thiosemicarbazone derivatives on steel [15–20]. To our knowledge this is the first time that thiosemicarbazone derivatives has been used as inhibitor for iron-base glassy alloy in aggressive media. *The purpose of this paper* is to clarify the corrosion of $\text{Fe}_{78}\text{B}_{13}\text{Si}_9$ metallic alloy in the absence and the presence of thiosemicarbazone derivatives in 0.2 M Na_2SO_4 solution, to establish a correlation between the inhibition efficiency of these organic compounds, molecular structure and the presence of substitutions on benzene ring and

* Corresponding author.

E-mail address: k_imran2000sa@yahoo.co.uk (K.M. Emran).

to propose a model for thiosemicarbazone derivatives adsorption on the amorphous surface.

2. Experimental

2.1. Inhibitors preparation

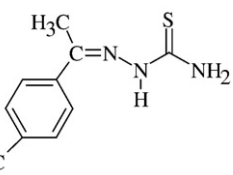
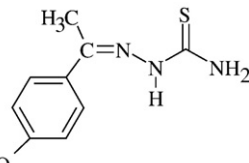
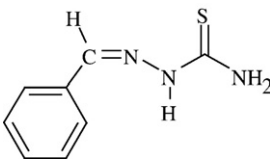
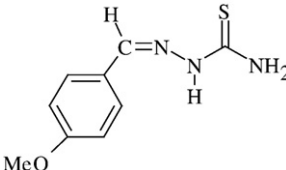
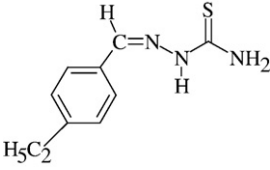
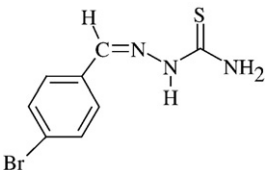
The thiosemicarbazone was prepared by condensation of the suitable carbonyl compound with thiosemicarbazide, (thioSCAz), (Aldrich) in the presence of an acid catalyst as follows [16,19], solution of either 4-methylacetophenone, 4-methoxyacetophenone, benzaldehyde, 4-methoxybenzaldehyde or 4-ethylbenzaldehyde in ethanol in the presence of 10% HCl was added to a solution of (thioSCAz) soluble in ethanol. The

reaction mixture was refluxed with stirring for 2 h. Upon cooling, the precipitated products were filtered off, washed with ethanol, ether and dried in vacuum, recrystallized twice from ethanol, and their melting points were recorded. The compounds' structure was confirmed by nuclear magnetic resonance (NMR). The structure, molecular weights and melting points for isolated products (A–F) are shown in Table 1.

2.2. Specimen and test solution preparation

In particular, Goodfellow $\text{Fe}_{78}\text{B}_{13}\text{Si}_9$ was used. Rounded specimens were cut from a foil (50 mm wide, 0.025 mm thickness) with working area (30 mm²) in all the experiments. The specimens were used without any mechanical polishing

Table 1
Symbol, structure, molecular weights and melting points for studied compounds

Symbol	Compound name and structure	Abbreviation	Molecular weight	Melting point (°C)
A	 4-Methyl acetophenone thiosemicarbazone	MeActioSCAzn	207.293	165–164
B	 4-Methoxy acetophenone thiosemicarbazone	MEActioSCAzn	223.293	183
C	 Benzaldehyde thiosemicarbazone	BndthioSCAzn	179.240	161.5
D	 4-Methoxy benzaldehyde thiosemicarbazone	MEBndthioSCAzn	209.266	176–177
E	 4-Ethyl benzaldehyde thiosemicarbazone	EtBndthioSCAzn	207.293	140
F	 4-Bromo benzaldehyde thiosemicarbazone	BrBndthioSCAzn	258.136	223

before each experiment. The electrochemical measurements were made on the bright face of the working electrode, the dull face being masked by chemically inert resin (Ciba, Araldite adhesive, England) which does not react with the chemical used as electrolyte. Each experiment was carried out with newly strip. The electrode was degreased with alcohol and rinsed several times with bi-distilled water and finally cleaned in an ultrasonic bath (Model LF2003, 50,160 Hz, Dal Trozzo) made in Italy. The electrode is connected to copper specimen holder and immersed in the test solution with out drying. The deaerated

0.2 M Na₂SO₄ solution containing 10% methanol was prepared using (BDH) sodium sulfate in bi-distilled water.

2.3. The electrochemical study

Electrochemical measurements have been achieved by connecting the electrochemical cell to ACM Gill AC and to a Samsung computer (Bridge DVD ASUS 8X max). Potentiodynamic polarization curves were performed with scan rate of 60 mV/min. Electrode potentials were measured with respect to a

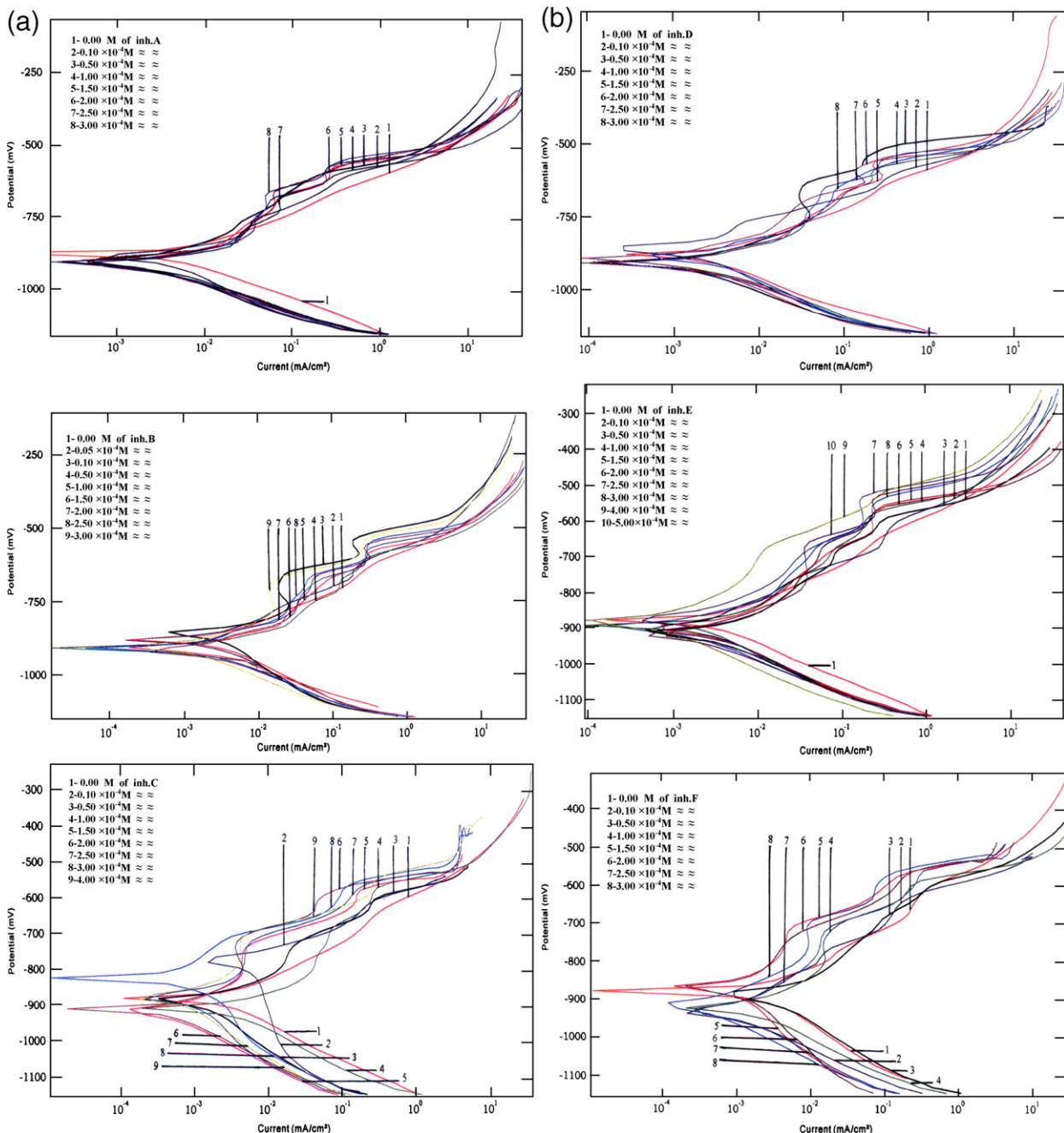


Fig. 1. Polarization curves of Fe₇₈B₁₃Si₉ metallic glass corrosion in 0.2 M Na₂SO₄ solution containing 10% MeOH in the absence and presence of different concentrations of inhibitors (A–F) at 30 °C.

Table 2

Inhibition percentages of $\text{Fe}_{78}\text{B}_{13}\text{Si}_9$ glassy alloy corrosion in 0.2 M Na_2SO_4 solution containing 10% MeOH in the presence of different concentrations of studied compounds (A–F) at 30 °C

C ($\text{M} \times 10^4$)	MeActhioSCAZn A		MEActhioSCAZn B		BndthioSCAZn C		MEBndthioSCAZn D		EtBndthioSCAZn E		BrBndthioSCAZn F	
	Inh. _p %	Inh. _{R_c} %	Inh. _p %	Inh. _{R_c} %	Inh. _p %	Inh. _{R_c} %	Inh. _p %	Inh. _{R_c} %	Inh. _p %	Inh. _{R_c} %	Inh. _p %	Inh. _{R_c} %
0.05	–	–	22.37	22.60	–	–	–	–	–	–	–	–
0.10	41.39	32.82	65.23	67.04	41.28	42.96	41.39	42.00	38.02	40.74	22.89	10.87
0.50	55.99	47.45	78.57	80.75	58.40	58.12	73.53	78.69	74.45	73.95	61.45	67.27
1.00	66.81	64.68	89.29	90.53	79.20	77.08	83.82	89.65	81.41	80.44	76.26	73.30
1.50	88.76	88.22	81.72	84.07	84.77	83.99	90.44	91.30	82.04	82.82	81.09	86.42
2.00	79.41	79.87	75.42	81.71	85.61	86.29	81.93	85.62	84.03	83.33	87.50	90.04
2.50	76.26	74.94	73.63	78.92	81.72	84.88	76.68	79.80	88.34	86.76	83.82	88.05
3.00	65.23	60.21	72.37	64.70	73.00	79.17	69.01	59.64	94.01	95.39	79.52	86.62
4.00	–	–	–	–	71.95	78.89	–	–	90.86	91.73	–	–
5.00	–	–	–	–	–	–	–	–	81.62	85.44	–	–

silver/silver chloride reference electrode with a Luggin capillary bridge and a platinum wire counter electrode. Impedance data was obtained in the frequency range of 0.5 Hz–10 kHz. The impedance diagram is presented as Nyquist plot where R is the real and $-j\omega$ (Z'') the imaginary part. All tests were performed at 30 °C.

2.4. Scanning electron microscopy (SEM)

For morphological studies, the samples were prepared and treated as described before and immersed in the test solution for 45 min, then SEM analysis was carried out using Leitz METALLUX 3 scanning microscope (WETZLAR, Germany), with magnification (500 \times).

3. Results and discussion

The polarization curves of $\text{Fe}_{78}\text{B}_{13}\text{Si}_9$ glassy alloy in deaerated 0.2 M Na_2SO_4 solution containing 10% MeOH at 30 °C are shown in Fig. 1. The obtained cathodic and anodic curves exhibited a Tafel-type behavior and the rate of the corrosion process is determined from the corrosion current density (i_{corr}) obtained by extrapolating the Tafel lines to the corrosion potential (E_{corr}) of the working electrode. Tafel

lines of approximately equal slope (b_a , b_c) are obtained. The corrosion inhibition efficiency (Inh._p%) are calculated by Eq. (1) and given in Table 2:

$$\text{Inh.}_p\% = \left(\frac{i_{\text{corr}}^0 - i_{\text{corr}}}{i_{\text{corr}}^0} \right) \times 100 \quad (1)$$

where i_{corr}^0 and i_{corr} denote corrosion current densities without and with inhibitor respectively.

All additives (A–F) behaved as mixed inhibitors, both anodic and cathodic reactions being polarized, the inhibition of $\text{Fe}_{78}\text{B}_{13}\text{Si}_9$ glassy alloy corrosion in test solutions proceeds predominantly under cathodic control in the case of compounds A, E and F. Inh._p% increase with inhibitor concentration reaching a maximum value. The cathodic curves are characterized by limiting diffusion current densities. Polarization curves at potentials higher than -200 to -300 mV vs $\text{AgCl}_s/\text{KCl}_{\text{aq}}$ in the presence of studied compounds the current–potential characteristics do not appear to change. This behavior may be described as a result of significant alloy dissolution leading to a desorption of the adsorbed film formed at the electrode surface in studied solution [21]. This potential can be defined as the desorption potential, which means that the thiosemi-carbazone compounds' adsorption depends on electrode potential. This behavior was reported for Diorthoaminophenoldisulfane (D-O-Anphs) up to -1000 mV vs (SCE) with $\text{Fe}_{82.2}\text{Cr}_{9.3}\text{P}_{5.9}\text{C}_{2.4}\text{Si}_{0.2}$ amorphous alloy in

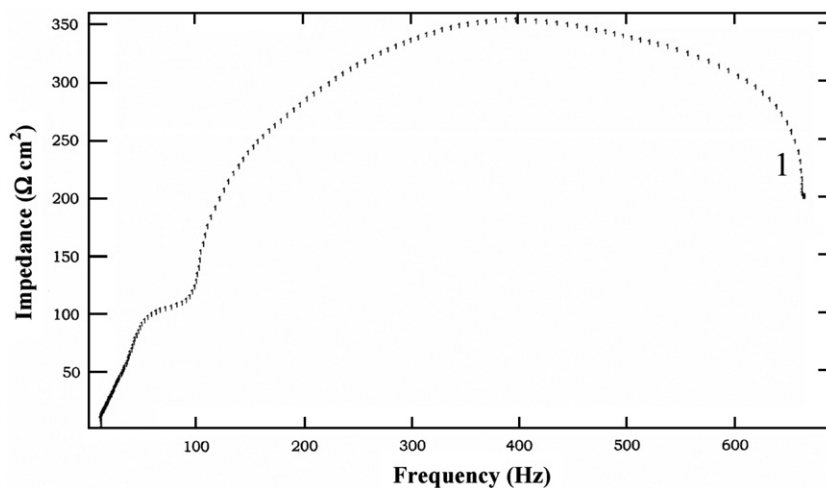


Fig. 2. Nyquist diagrams of $\text{Fe}_{78}\text{B}_{13}\text{Si}_9$ metallic glass corrosion in 0.2 M Na_2SO_4 solution containing 10% MeOH at 30 °C.

1.0 M HCl [22] and up to -300 mV vs (SCE) with FeBSi amorphous alloy in 1.0 M HCl [23] and for 3-amino-1,2,4-triazole (3-An(Az)3) up to -200 mV vs (SCE) with $\text{Fe}_{80}\text{B}_{13}\text{Si}_{3.5}\text{C}_{3.5}$ amorphous alloy in the same

media [24]. The Tafel slopes were not to be affected to any great extent, so the mechanism of both anodic and cathodic reactions does not change by addition of studied compounds in test solutions.

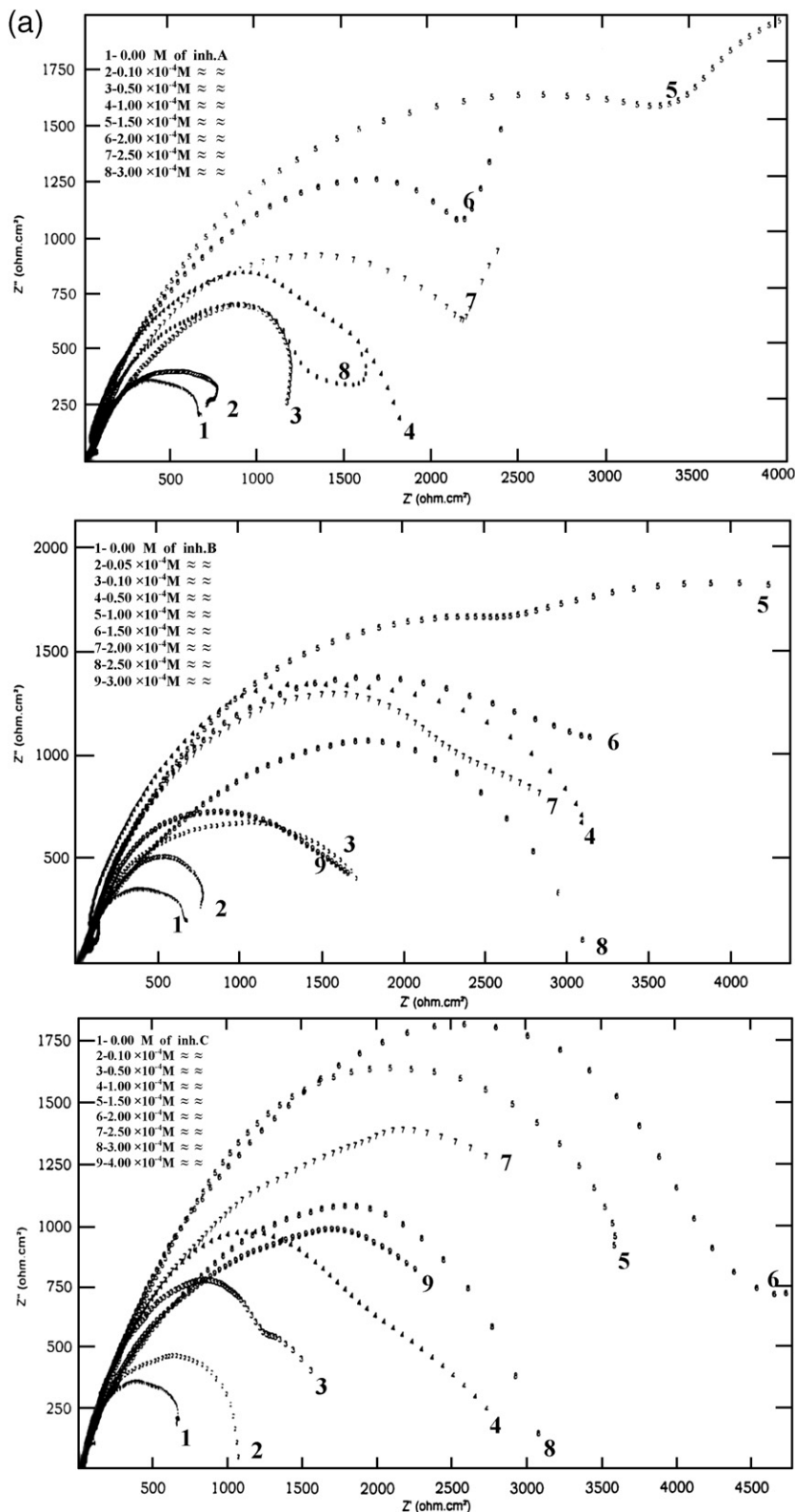


Fig. 3. a. Nyquist diagrams of $\text{Fe}_{78}\text{B}_{13}\text{Si}_9$ metallic glass corrosion in 0.2 M Na_2SO_4 solution containing 10% MeOH in the absence and presence of different concentrations of inhibitors (A–C) at 30 °C. b. Nyquist diagrams of $\text{Fe}_{78}\text{B}_{13}\text{Si}_9$ metallic glass corrosion in 0.2 M Na_2SO_4 solution containing 10% MeOH in the absence and presence of different concentrations of inhibitors (D–F) at 30 °C.

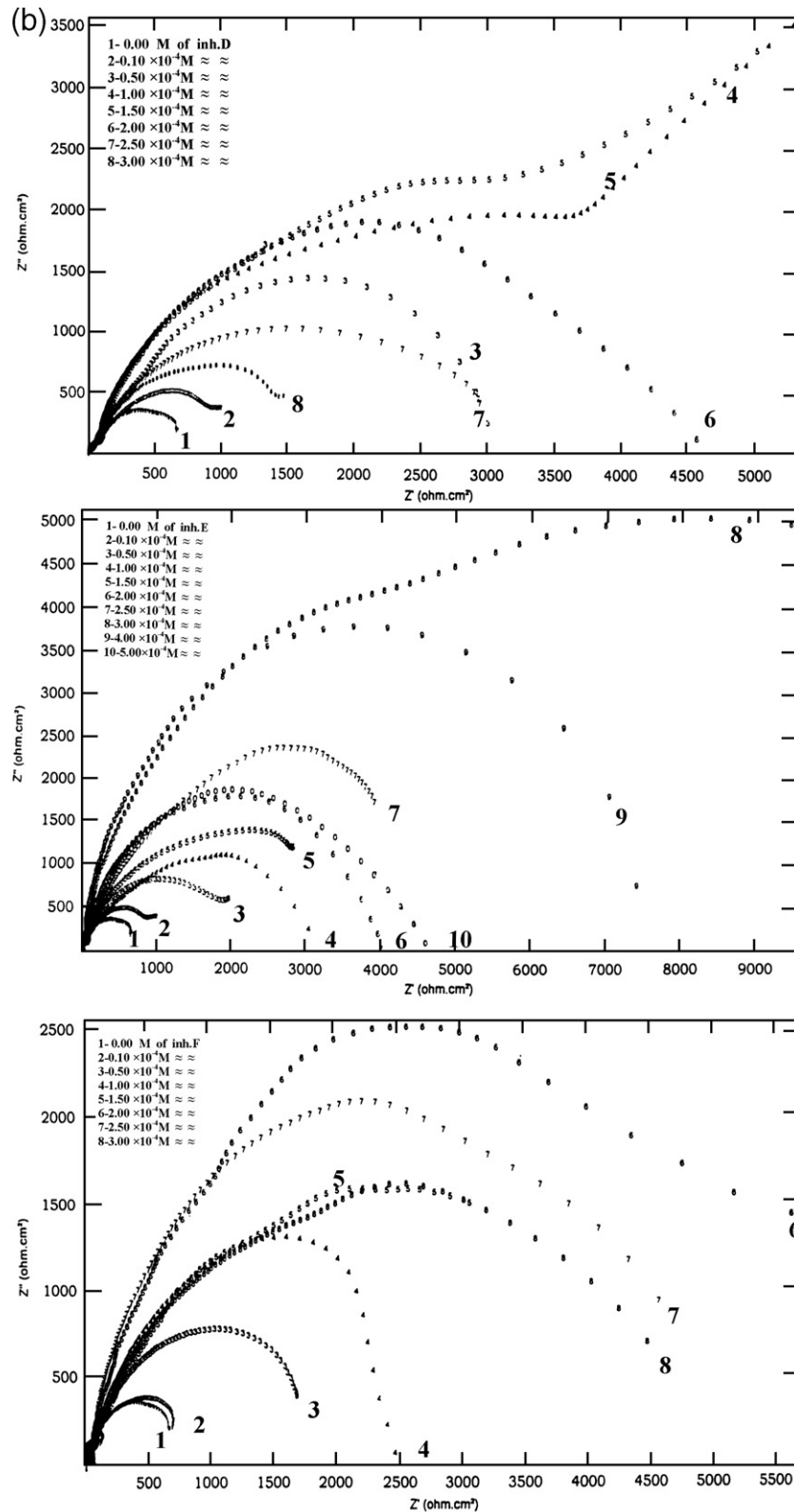


Fig. 3 (continued).

The obtained Nyquist plots (Cole–Cole plots) of $\text{Fe}_{78}\text{B}_{13}\text{Si}_9$ glassy alloy in 0.2 M Na_2SO_4 solution consists of two capacitive loops, Fig. 2. The high-frequency (HF) loop, the smaller one, can be attributed to the film formation at the alloy surface, while the low-frequency (LF) loop, the larger one can be attributed to charge

transfer reaction. The EIS spectra for test compounds (Fig. 3) sometimes consist of two capacitive loops, one at HF and the other at LF, or sometimes present one depressed semicircle with a long or short tail at LF which is with respect to the semicircle representing the inhibitor film.

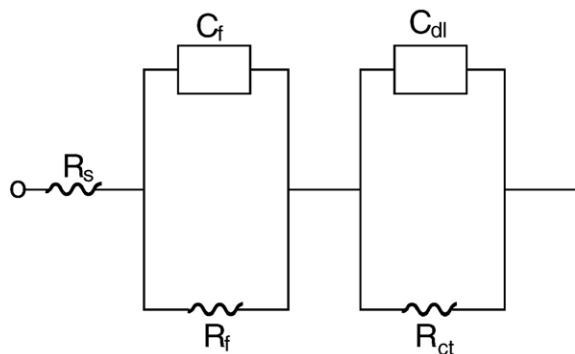


Fig. 4. Equivalent circuit (EC) model for the spectra exhibiting two capacitive time constants, R_s , solution resistance, R_f , film resistance, C_f , film capacitance, R_{ct} , charge transfer resistance, C_{dl} , double layer capacitance.

In the first case that the glassy alloy exhibits a HF capacitive loop in addition to a LF capacitive loop suggested that some sort of film exists on this alloy in the studied solution and the corrosion reaction is under both charge transfer and diffusion control, similar behaviors were obtained by Seshu et al. [25] and Morad [26]. The equivalent circuit (EC) model in this case is shown in Fig. 4.

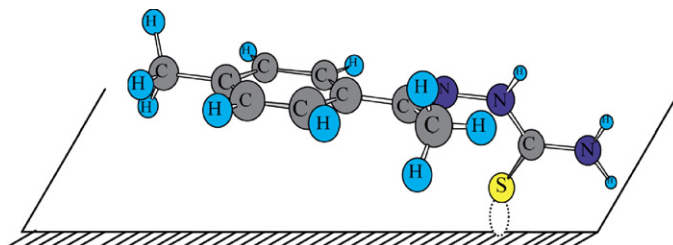
On the other hand, the Nyquist plots for the inhibition test presents one depressed semicircle with a tail at the low-frequency region, which can sometimes merge with the charge transfer loop. This behavior indicates that the diffusion process of ions takes place on the electrode after the addition of corrosion inhibitor and the existence of a protective porous film on metal surface, in which the diameters of the pores control the diffusion ions through the film [27]. Figs. 5 and 6 give a schematic diagrams of the metal surface covered by porous films and the simplified equivalent model for the previous system respectively.

The charge transfer resistance, R_{ct} (limiting zero frequency value of the real part of the complex impedance), values are calculated from the difference in the impedance at lower and higher frequencies. The inhibition percentage efficiencies of the corrosion rate ($\text{Inh. } R_{ct} \%$) in the presence of different concentration of thiosemicarbazone derivatives are calculated by Eq. (2) and given in Table 2:

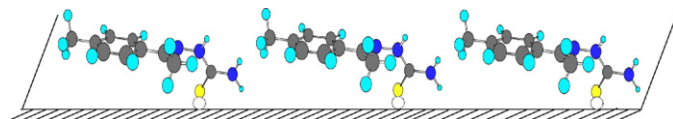
$$\text{Inh. } R_{ct} \% = \left(R_{ct0}^{-1} - R_{ct}^{-1} / R_{ct0}^{-1} \right) \times 100. \quad (2)$$

As shown in Fig. 3, R_{ct} value increases with concentration increase of compounds and there after its value decreases with increase in the concentration of thiosemicarbazones. This may be due to the gradual replacement of the water molecules by the adsorption of the compound molecules on the alloy surface [28]. C_{dl} values are considerably reduced due to the decrease in local dielectric constant and/or an increase in the thickness of electrical double layer, which suggests that the inhibitor molecules function by adsorption at the metal–solution interface [29]. Inhibition efficiency increase up to critical inhibitor concentration was found in agreement with the polarization study. The inhibition efficiency for the corrosion of $\text{Fe}_{78}\text{B}_{13}\text{Si}_9$ alloy in test solution in the presence of thiosemicarbazones may be explained on the same basis, that at lower concentration of thiosemicarbazones the adsorption intermediate formed leading to high values of inhibition efficiency and blocking of most of the active sites on the alloy surface occurred due to increased coverage (θ). Moreover the increase of inhibition with the increase of concentration of the studied thiosemicarbazones may be explained as the adsorption resulting from increase in the electron density at the center ($\text{C}=\text{S}$) by suitable substitution of a terminal

hydrogen in hydrazine and/or thiamino groups of the thiosemicarbazide molecule. When the different models of thiosemicarbazone derivatives' adsorption are considered, the following model is possible:



This model is stable and preferred since the covered fraction of the surface is high, even at low concentrations. This adsorption model is favored by establishing (donor–acceptor) links between the empty d orbitals of Fe and the pairs of free electrons on S atom. The increase in the surface coverage with the increases in concentration may be illustrated by the following representation:



These decreases are the result of presence of H_2S which is one of the by-products of reduction of thioureas. The ions HS^- or S^{2-} compete very favorably for sites on the metals to form “Fe–S” centers on the surface which would then dissolve easily in the test solution promoting more rapid corrosion [30].

4. Adsorption isotherm

The obtained data in Table 2 are used to determine the suitable isotherm fitting the surface coverage relation with inhibitor concentration from polarization and impedance results. The kinetic–thermodynamic model [31] at 30 °C gave good fitting of the obtained data. The slope of the lines is representing y (the number of inhibitor molecules occupying a single active site). The intercept is $\log \kappa$ and $(1/y)$ gives the number of active sites occupied by a single inhibitor

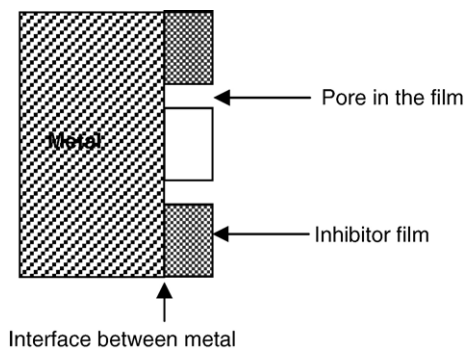


Fig. 5. A schematic diagram of the metal covered by porous inhibitor films.

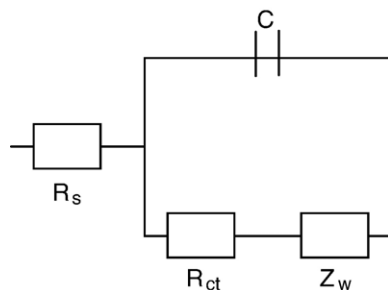


Fig. 6. Equivalent circuit model for the metal covered by porous inhibitor films, R_s , solution resistance, R_{ct} , charge transfer resistance, Z_w , Warburg impedance.

molecular. The binding constant K for the adsorption process is equal to $\kappa^{1/y}$:

$$\log [\Theta/1 - \Theta] = \log \kappa + y \log C_{inh} \quad (4)$$

where κ is a constant and is related to the binding constant, by the following relationship:

$$K = \kappa^{1/y}. \quad (5)$$

The value of K is related to the standard free energy of adsorption by the following equation:

$$K = 1/55.5 \exp(-\Delta G_{ads}^0/RT). \quad (6)$$

The value 55.5 is the concentration of water in the solution in mol L⁻¹, and R is the gas constant and T is absolute temperature. Table 3 gives the adsorption parameters obtained from kinetic–thermodynamic model isotherm. According to the structure of molecules in Table 1 the studied compounds can be classified into two groups:

- i. Acetophenone thiosemicarbazone compounds including compounds A and B.
- ii. Benzaldehyde thiosemicarbazone and its *p*-substituted derivatives which includes compounds C, D, E and F.

For group (i) the inhibition efficiency from both electrochemical measurements at 10⁻⁴ M is as follows:

B>A

and for group (ii) at 10⁻⁴ M follows the following order:

D>E>C>F.

This clearly indicates that the strength of electrical interactions by adsorbing molecules and surface of the metal increases in the same order noticed previously.

The results also show that the number of active sites is approximately equal to the unity indicating that the adsorption process takes place by the occupation of one active site per a single inhibitor molecule in agreement with the suggested model for studied compounds. Values of ΔG_{ads}^0 are a characteristic feature of strong adsorption. In general, the negative values of the free energy of adsorption indicate the spontaneous adsorption of inhibitors on the alloy [19].

5. Morphological study

From the comparison between Fig. 7a (as-received), the surface contains only trace produced during the parallel flow casting of the material from the liquid to solid state and Fig. 7b (specimen immersed in test solution) at 30 °C after 45 min, general corrosion with large shallow pits may be caused by SO₄²⁻ ions at the amorphous surface alloy, and an evidence of a severe attack of the alloy by Na₂SO₄ occurred. The presence of 10⁻⁴ M of each studied inhibitor (A–F) Fig. 7c–h, the amorphous surface may be covered by compact inhibitor film on the surface in the presence of inhibitors as suggested before which reduce the corrosion process. This means that inhibitors have strong tendency to adhere (strong adsorption) on the amorphous surface. Visual observation supports deductions made from both polarization and impedance studies.

6. Effect of structure of the inhibitor molecules on the inhibition efficiency

In general the extent of adsorption of different inhibitors at a fixed concentration will depend on the surface area of the inhibitor molecules, number and position of active center such N, S and O atoms along with delocalized π electron density on the aromatic rings. It was found that thiosemicarbazide and its derivatives act as mixed adsorption type inhibitors, with adsorption resulting from increase in the electron density at the center by suitable substitution of a terminal hydrogen atom in hydrazino and/or thiamino groups of the thiosemicarbazide molecule. Studied compounds can be divided according to their structure into two parts.

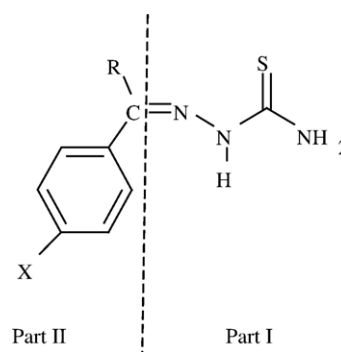


Table 3

Binding constant, number of active sites and change in free energy values obtained from the kinetic–thermodynamic model for studied compounds (A–F) in 0.2 M Na₂SO₄ containing 10% MeOH at 30 °C

Symbol	Kinetic–thermodynamic model					
	(Polarization)			(Impedance)		
	1/y	K (M ⁻¹)	ΔG_{ads}^0 (kJ mol ⁻¹)	1/y	K (M ⁻¹)	ΔG_{ads}^0 (kJ mol ⁻¹)
A	1.33	46,066.11	-37.16	1.15	32,842.56	-36.30
B	1.04	96,284.24	-39.01	0.9955	98,448.65	-39.07
C	1.32	53,999.21	-37.55	1.366	53,588.89	-37.53
D	1.08	66,546.72	-38.08	0.9822	73,431.41	-38.33
E	1.23	55,346.55	-37.61	1.250	60,582.09	-37.84
F	0.973	30,705.56	-36.130	0.7119	24,674.14	-35.58

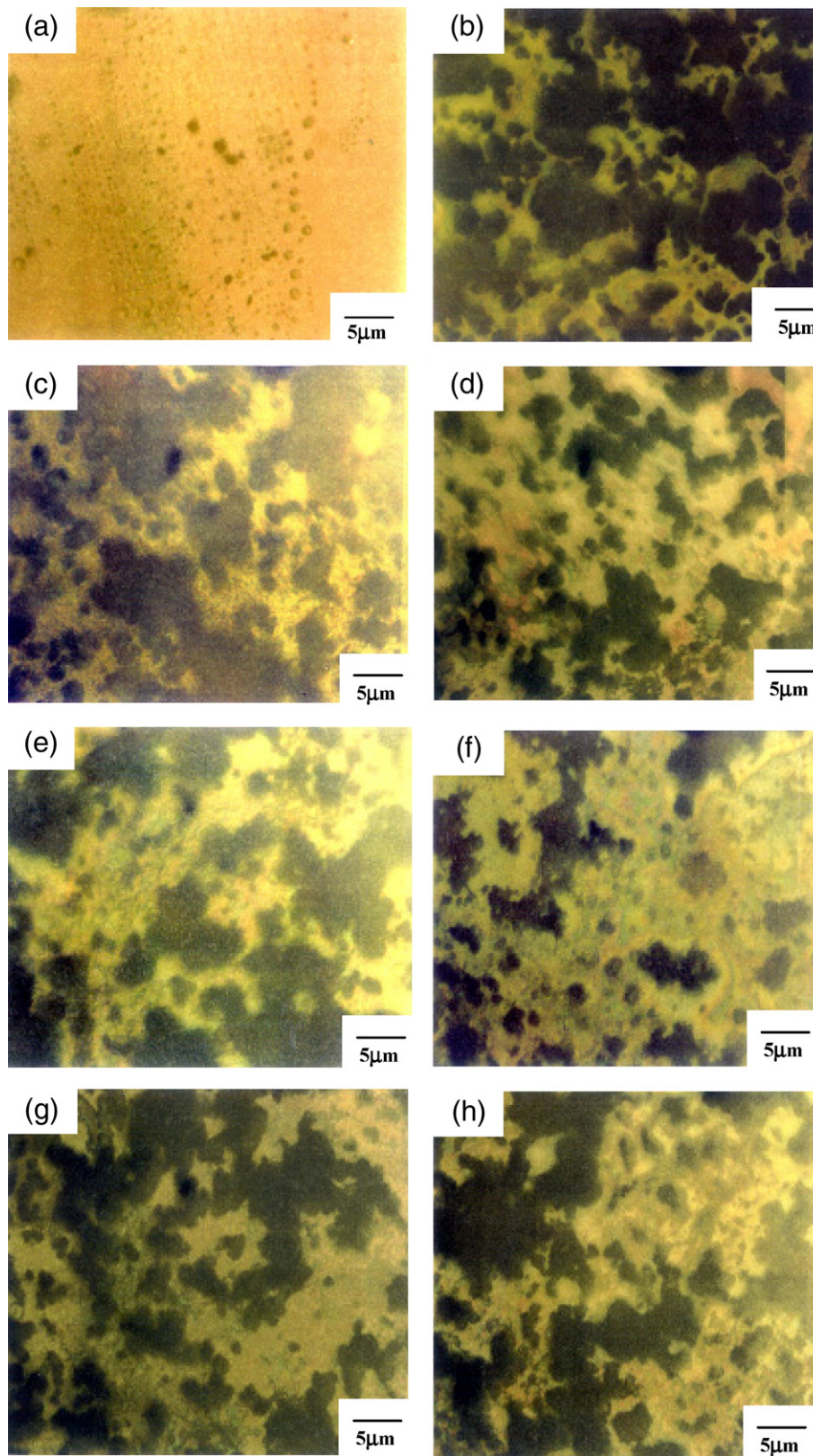


Fig. 7. (a) Optical micrographs (500 \times) of as-received surface of $\text{Fe}_{78}\text{B}_{13}\text{Si}_9$ glassy alloy, (b) optical micrographs (500 \times) of $\text{Fe}_{78}\text{B}_{13}\text{Si}_9$ glassy alloy after 45 min immersion in 0.2 M Na_2SO_4 solution containing 10% MeOH at 30 $^\circ\text{C}$ in the presence of 0.0 M of inhibitor, (c) in the presence of 10^{-4} M of Inh. A, (d) in the presence of 10^{-4} M of Inh. B, (e) in the presence of 10^{-4} M of Inh. C, (f) in the presence of 10^{-4} M of Inh. D, (g) in the presence of 10^{-4} M of Inh. E and (h) in the presence of 10^{-4} M of Inh. F.

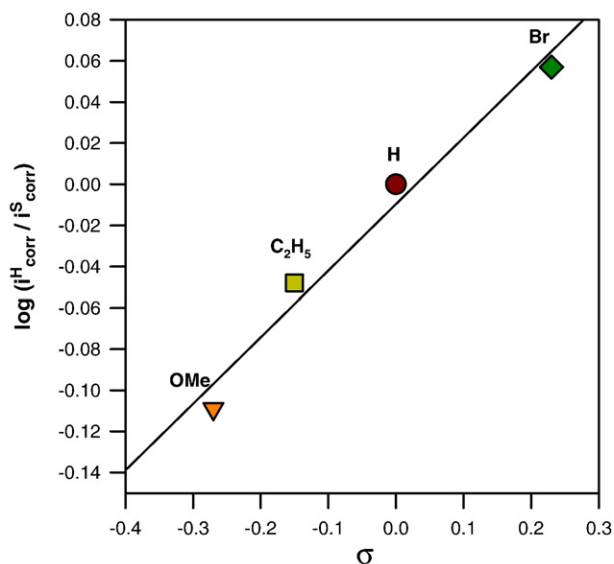


Fig. 8. The relationship between ($\log i_{\text{corr}}^{\text{S}}/i_{\text{corr}}^{\text{H}}$) and Hammett constants of compounds (C, D, E and F) at 10^{-4} M in 0.2 M Na_2SO_4 solution containing 10% MeOH at 30 °C.

As seen in Table 1, all compounds are sharing in part I and are different in part II. Moreover as discussed before these compounds can be divided into two groups: group (i) where $\text{R}=\text{CH}_3$ and $\text{X}=\text{CH}_3$ or MeO and in group (ii) where $\text{R}=\text{H}$ and $\text{X}=\text{H}$, MeO, C_2H_5 or Br. The lone pairs of electrons on the N and S atoms, the azomethene ($-\text{CH}=\text{N}$) double bonded and those of benzene ring will give a good protection efficiency. In the case of compounds A and B the higher efficiency of B (89.29%) at 10^{-4} M compared to A (66.18%) at the same concentration of each of them due to an increase in the electron density on adsorption center by electron-donating group (MeO) on the benzene ring beside the presence of methyl group. This enhancement in inhibition efficiency is conceivable in the light of better electron-donating property of (MeO) than that of (CH_3) group. Similar observation had been reported by Abd-El-Nabey et al. [16]. Quraishi et al. have also explained the higher inhibition efficiency of methoxy benzothiazole (MEthioAz) [32] and methoxy dithiobiurd (ME-DthioBt) [33] as compared with methyl substitution of these compounds on the basis of the inductive effect.

BndthioSCAzn (C), in which (R and $\text{X}=\text{H}$) may be adsorbed by donating a pair of unshared electrons to an unoccupied orbital of iron in the alloy. The adsorption left the rest of the molecule (tail) to be interacted through Van der Waals force, forming a hood covering the adsorption functional group.

There is reason to believe that the larger the number of delocalized electrons, the more stable is the structure and the more is the charge density on the unsharing atom (in this case S) and hence the large is the extent of adsorption i.e. high value for Θ [23].

In group (ii) the difference in the efficiency is referred to the molecular structure effect, to the rigidity of π -delocalized system of C, D, E and F, besides, the presence of substitutions on benzene ring in compounds (D–F), may cause the increasing or decreasing of the electron density on center of adsorption, and leading to an easier electron transfer from the functional group

($\text{C}=\text{S}$) to the metal, producing greater coordinate bonding and hence different adsorption and inhibition efficiency. The superior performance of compound D (83.82%) as corrosion inhibitor compared with compounds E (81.30%) and C (79.20%) at 10^{-4} M of each of them can be attributed to the presence of the effective electron releasing group (MeO) leading to greater adsorption of methoxy substituted thiosemicarbazone (D), on the iron-base alloy surface than ethyl substituted derivative (E), and the unsubstituted compound (C). The lower value of the efficiency for compound F (76.26%) as compared with the unsubstituted compound (C) may be attributed to the effect of the bromo atom (electron with drawing inductive effect) which decreases the electron availability on the reaction site and causes less adsorption of bromo derivative (F) on the alloy surface, this trend has been reported by Quraishi et al. [33].

7. Hammett's equation

The corrosion data for group (ii) demonstrates well the effect of the electron density on ($\text{C}=\text{S}$) on the inhibition efficiency. This is done by substituting the hydrogen atom in *para* position of benzene ring by either electron-donating groups, e.g. MeO and C_2H_5 or electron with drawing group, e.g. Br. The effect can be evaluated quantitatively through a correlation between the substituting constant, σ , and the current density. According to the linear free energy relationships (LFER) or Hammett's equation [34].

$$\log (i_{\text{corr}}^{\text{S}}/i_{\text{corr}}^{\text{H}}) = \sigma \rho \quad (7)$$

where $i_{\text{corr}}^{\text{H}}$ and $i_{\text{corr}}^{\text{S}}$ are the corrosion current densities in the absence and presence of the substituting respectively. ρ is the reaction constant and σ is the substituting constant [35]. Those substitutions which attract electrons from the reaction center are assigned positive σ values and those which are electron donating have negative σ values. Thus, σ is a relative measure of the electron density at the reaction center. The slope of the plot \log (current density) vs. σ is ρ , and its sign indicates whether the process is inhibited by an increase or a decrease of electron density at the electron center. The magnitude of ρ indicates the relative sensitivity of inhibition process to electron effects. Fig. 8 shows that the benzaldehyde thiosemicarbazone derivatives (C–F) gave good correlation. The small positive slope ($\rho=0.32$) shows a weak dependence of the adsorption character of the reaction center on the electron density of the ring, with electron releasing substitutions increasing inhibition.

8. Conclusion

Thiosemicarbazone compounds function as mixed inhibitors against the corrosion of the $\text{Fe}_{78}\text{B}_{13}\text{Si}_9$ alloy in 0.2 M Na_2SO_4 solution containing 10% MeOH. The inhibition efficiency increases with the increase of inhibitor concentration and attains a maximum value. Each thiosemicarbazone derivatives molecule occupied one active site at the investigation concentration. Negative values of ΔG_{ads}^0 indicated spontaneous adsorption of the inhibitor molecules on the alloy surface. Optical micrograph

studies of $\text{Fe}_{78}\text{B}_{13}\text{Si}_9$ in the absence and presence of the inhibitors significantly reduce the reactions between the test solution and amorphous surface.

References

- [1] M.G. Fantana, Corrosion Engineering, McGraw-Hill International Edition, 3th edition, Materials Letters, New York 1987.
- [2] K. Hashimoto, T. Masumoto, in: H. Herman (Ed.), Ultrarapid Quenching of Liquid Alloy, Academic Press, New York 1981.
- [3] K. Hashimoto, in: F.E. Luborsky (Ed.), Amorphous Metallic Alloys, Butterworths, London 1983.
- [4] J.J. Gilman, in: R.L. Ashbrook (Ed.), Rapid Solidification Technology Source Book, ASM, Metals Park, OH 1983.
- [5] K. Mohri, IEEE Trans. Mag., MAG 20 (1984) 942.
- [6] C.H. Smith, K. Nathasingh, in: J. Thompson (Ed.), Soft Magnetic Materials, University College, Cardiff 1985, p. 300.
- [7] H. Warlimont, Rapidly quenched metals, in: S. Steeb, H. Warlimont (Eds.), Proc. 5th Int. Conf., Amsterdam 1985, p. 1599.
- [8] K. Habib, A. Abdullah, Corrosion 50 (7) (1994) 531.
- [9] M. Naka, K. Hashimoto, T. Mosumoto, J. Jpn. Inst. Metals 38 (1974) 835.
- [10] I.B. Singh, R.S. Chaudhary, T.K.G. Namboodhiri, Mater. Sci. Eng. 83 (1986) 123.
- [11] K. Habib, R. Nessler, K. Moore, Corrosion 49 (8) (1993) 619.
- [12] S. Pang, T. Zhang, K. Asami, A. Inoue, J. Mater. Res. 17 (3) (2002) 701.
- [13] J.X. Guo, J.X. Li, L.J. Qiao, K.W. Gao, W.Y. Chu, Corros. Sci. 45 (4) (2003) 735.
- [14] G. TrabANELLI, V. Corassiti, in: M.G. Fontana, R.W. Stachle (Eds.), Advances in Corrosion Science and Technology, Plenum Press, New York 1970.
- [15] B. Donnelly, T.C. Downie, R. Grzekowiak, D. Short, Corros. Sci. 14 (10) (1974) 597.
- [16] B.A. Abd El-Nabey, N. Khalil, M.A. Shaban, M. Nasr, E. Khamis, G.E. Thompson, Proc. 6th Eur. Sym. on Corrosion Inhibitors, Ferrara Italy 1985, p. 205.
- [17] E. Khamis, B.A. Abd El-Nabey, Corros. Prev. Control 37 (5) (1990) 127.
- [18] B.I. Ita, O.E. Offiong, Mater. Chem. Phys. 48 (1997) 164.
- [19] E. Khamis, M.A. Ameer, N.M. Al-Andis, G. Al-Senani, Corrosion 56 (2) (2000) 127.
- [20] M.A. Quraishi, D. Jamal, R.N. Singh, Corrosion 58 (3) (2002) 201.
- [21] R.S. Chaudhary, T.K.G. Namboodhiri, I.B. Singh, A. Kumar, Br. Corros. J. 24 (4) (1989) 273.
- [22] M. Etman, A. Elkholy, J. Aride, T. Biaz, S. Kertit, J. Chim. Phys. 86 (2) (1989) 347.
- [23] S. Kertit, J. Aride, A. Ben-Bachir, A. Srhiri, M. Etman, J. Appl. Electrochem. 23 (1993) 1132.
- [24] S. Kertit, F. Chaouket, A. Srhiri, M. Keddami, J. Appl. Electrochem. 24 (1994) 1139.
- [25] B. Seshu, A.K. Bhatnagar, A. Venugopal, V.S. Raja, J. Mater. Sci. 32 (1997) 2071.
- [26] M.S. Morad, Corros. Sci. 42 (2000) 1307.
- [27] Y. Chen, T. Hong, M. Gopal, W.P. Jepson, Corros. Sci. 42 (2000) 979.
- [28] E. Khamis, N. Al-Andis, Mater. wiss. Werkst. tech. 33 (2002) 1.
- [29] F. Bentiss, M. Traisnel, M. Lagrenee, J. Appl. Electrochem. 31 (2001) 41.
- [30] A.C. Makrides, N. Hackerman, Ind. Eng. Chem. 47 (1955) 1773.
- [31] E. Khamis, M.A. Ameer, N.M. Alandis, G. Al-Senani, Corrosion 56 (2) (2000) 127.
- [32] M.A. Quraishi, M.A.W. Khan, M. Ajmal, S. Muralidharan, S.V.K. Iyer, J. Appl. Electrochem. 26 (1996) 1253.
- [33] M.A. Quraishi, J. Rawat, M. Ajmal, J. Appl. Electrochem. 30 (2000) 745.
- [34] L.P. Hammett, Physical Organic Chemistry, 2nd ed, McGraw-Hill, Kogokusha, 1970.
- [35] J. March, Advanced Organic Chemistry, 4th, John Wiley and Sons, Inc., New York, 1992.